Hygrothermal ageing behaviour of a glass/epoxy composite used in wind turbine blades

Barcelos Carneiro M Rocha, I.; Raijmaekers, S; Nijssen, R. P.L.; van der Meer, F. P.; Sluys, L. J.

DOI
10.1016/j.compstruct.2017.04.028

Publication date
2017

Document Version
Accepted author manuscript

Published in
Composite Structures

Postprint of Composite Structures
Volume 174, 15 August 2017, Pages 110–122
Link to formal publication (Elsevier): https://doi.org/10.1016/j.compstruct.2017.04.028

Hygrothermal ageing behaviour of a glass/epoxy composite used in wind turbine blades

I. B. C. M. Rocha[a,b,*], S. Raijmaekers[a], R. P. L. Nijssen[a], F. P. van der Meer[b], L. J. Sluys[b]

[a]Knowledge Centre WMC, Kluisgat 5, 1771MV Wieringerwerf, The Netherlands
[b]Delft University of Technology, Faculty of Civil Engineering and Geosciences, P.O. Box 5048, 2600GA Delft, The Netherlands

Abstract

In this work, a glass/epoxy material system applied in wind turbine blades was used to evaluate degradation processes induced by water ingression. Composite and neat epoxy specimens were conditioned in demineralised water at 50°C for 4800h and tested quasi-statically and in fatigue. Comparing results from mechanical tests in composite specimens, significant degradation was found, with up to 36% lower static shear strength and three orders of magnitude shorter fatigue life. For neat epoxy specimens, a lower degree of degradation was observed, with up to 17% lower tensile and bending moduli and strength. Specimens dried after having been immersed were also tested. For composite samples, recovery of shear stiffness and strength was incomplete. For neat resin, stiffness and bending strength were completely recovered but a decrease in the strain at failure was observed. It is hypothesised from differences in magnitude and reversibility of degradation between composite and neat resin that matrix degradation is accompanied by high differential swelling stresses and damage to the fibre/matrix interface in composites. The damage due to moisture ingression and the subsequent changes in failure behaviour are further investigated through thermal analysis (DSC, DMA) and optical microscopy.

Keywords: Environmental degradation, Polymer-matrix composites (PMCs), Interface/Interphase, Mechanical testing

1. INTRODUCTION

Research on material usage optimization for wind turbine blades has been on the rise in the past years, as designers seek ways to optimise the use of composite materials that comprise the main load bearing structures in blades. This can be done by reducing design uncertainty, consequently allowing for lighter blades

*Corresponding author. Tel. +31 0227 504928
Email address: i.barcelos@wmc.eu (I. B. C. M. Rocha)

with a higher degree of reliability. In this regard, one of the promising ways to reduce uncertainty is to better understand material behaviour and its interaction with its service environment. Rotor blades are designed to withstand extreme environmental conditions, particularly in offshore wind farms. Such a service environment usually involves high/low temperature cycles, wet/dry periods, UV radiation exposure and erosion by sand and other particles. Although each of these effects may impact the mechanical properties of composite materials, the combined influence of temperature and moisture ingression, particularly in combination with fatigue loading, is regarded as the most critical one and is the focus of this paper.

Despite the vast body of literature on the subject, hygrothermal ageing of polymers and composites is still a challenging research topic, and not fully understood. This lack of understanding is partly due to the fact that hygrothermal ageing is a complex combination of physical and chemical phenomena that may operate at different time scales [1]. Furthermore, it affects each of the involved material components (fibre, matrix and interface) differently [2] and the incurred damage strongly depends on the chemical composition of the materials involved as well as on the exposure environment. Lastly, interaction with other ageing processes, such as polymer relaxation (physical ageing) [3] and oxidation [4], can make results difficult to interpret.

Upon exposure to humid environments, polymer-matrix composites tend to absorb water molecules through a combination of diffusion and capillary action. Some of these molecules become chemically attached to hygrophilic polymer chains through hydrogen bonds, while others fill the free volumes in the polymer network [5]. If the medium becomes cracked, additional uptake is observed as the water fills the newly developed empty spaces. The absorption behaviour is highly dependent on the exposure temperature and humidity, both in terms of maximum uptake and diffusion speed [6]. At shorter exposure times, such dependency is well predictable and thus well documented in literature. However, at longer times, secondary effects such as fibre/matrix interface cracking [7], leaching [8] and polymer relaxation [9] come into play, and many uncertainties remain regarding the resultant material behaviour.

Once inside the material, water molecules tend to plasticize the resin, lowering its glass transition temperature (T_g) [10], and cause swelling. Additionally, the water causes the matrix to swell. Because fibres usually do not take any water, high stresses can occur due to differential swelling [11]. Water can also chemically interact with polymer chains (hydrolysis) [12], fibres (stress corrosion) [13] and fibre sizing [2]. It is important to note that chemical processes tend to be irreversible and persist even after the material is dried. Physical processes such as plasticization are generally reversible, particularly at short exposure times, but may also be partially irreversible if stronger bonds between water molecules and polymer chains are formed [5] or unbound plasticizing segments are leached from the network [8].

Most authors attempt to use water uptake results in order to discern the degradation mechanisms at play. The observed uptake is usually Fickian for neat resin, although deviations from this behaviour have been noted in literature [2, 9, 14], being mainly attributed to relaxation processes or hydrolitic chemical reactions. For composites, Fickian behaviour is initially observed but significant deviations appear at longer exposure times [10, 14, 15]. Although such deviations may provide indications of additional damage mechanisms at the fibre/matrix interface, few works [2, 16, 17] attempt to explicitly compare composite specimens with their unreinforced resin counterparts.

Multiple works also investigate material degradation after water absorption through mechanical tests [2, 11, 16, 18]. Fatigue life reduction is still not systematically investigated, and while some authors report significant degradation [1, 19, 20], others do not observe noticeable changes after water ingression [21]. Finally, very few authors have performed tests on specimens dried after being saturated [17], which allows for explicitly isolating the effects of irreversible degradation mechanisms.

The objective of this work is to analyse damage processes induced by hygrothermal ageing on an epoxy system reinforced with E-Glass fibres representative of the material used in wind turbine blade design. The water ingression process was tracked and a finite element modelling approach combined with an optimisation-based parameter identification technique is used to identify Fickian and non-Fickian absorption phases and determine the diffusivity parameters. In order to evaluate the combined effect of interface and matrix degradation, ILSS (Interlaminar Shear Strength) short-beam specimens were tested quasi-statically and in fatigue. Furthermore, in an attempt to isolate the contribution of matrix degradation, neat epoxy specimens were also conditioned and tested. In order to isolate the irreversible part of the degradation due to water immersion, a combination of mechanical and thermal tests was also conducted on specimens dried after saturation and on moisture-free isothermically conditioned specimens. Lastly, the material damage processes incurred during the immersion process and the consequent changes in failure modes observed in the mechanical tests were investigated through the use of optical microscopy. The combination of wet and dry tests on composite and resin specimens allows for a reconstruction of the chronology of the complex process of ageing in composites.

2. Experiments

2.1. Materials

The resin system used is the Momentive EPIKOTE RIMR 135 / EPIKURE RIMH 1366, consisting of a monomer (70-100% 4,4-Isopropylidenediphenol-Epichlorohydrin Copolymer and 0-30% 1,6-Hexanediol

Diglycidyl Ether) and a hardener (25-50% Alkyletheramine, 20-25% Isophoronediamine and up to 20% Aminoethylpiperazine) [22] mixed in a 100:30 ratio in weight. For the composite panels, a unidirectional fabric composed of PPG Hybon 2002 glass fibre rovings (95% of the fibres oriented at 0° with 5% composing stability rovings oriented at 90°) was used. This glass/epoxy material is one of the most commonly used systems to compose the main load bearing structures of wind turbine blades.

Composite panels with 4 and 6 plies (3mm and 4.5mm thick, respectively) and neat resin panels of 4mm thickness were manufactured through vacuum infusion molding. The curing cycle consisted of 2h at 30°C and 5h at 50°C, followed by postcuring for 10h at 70°C. Specimens were cut from the panels using a CNC milling machine. Composite specimens were 0° unidirectional short-beams with geometry according to the ISO 14130 standard. As for neat epoxy specimens, dog-bone specimens according to specimen geometry 1B of the ISO 527-2 standard and flexural beams according to the ISO 178 standard were used.

2.2. Sample Conditioning

An overview of the applied conditioning procedures can be seen in Figure 1, where each point marked in the curve represents a point in time when specimens were removed from conditioning and tested. In accelerated ageing studies, the choice of the reference (unaged) state can be a complex one. For the particular case of hygrothermal ageing, the ideal reference state would be a moisture-free one, allowing for the correct determination of the maximum water uptake and degree of irreversible material degradation through the redrying of saturated specimens. However, unless such state is achieved by drying (and redrying) the material at room temperature, which can be prohibitively time-consuming, interactions with other ageing processes such as physical ageing and oxidation are difficult to avoid when the material is dried at higher temperatures. These additional ageing processes can in turn modify not only the material mechanical properties [4, 17] but also properties related to the diffusion process itself such as maximum uptake, diffusivity and swelling coefficient [3, 9].

In this work, the *Unaged* state was defined by seeking a balance between a moisture-free state and an unmodified polymer chain structure. This was achieved by drying all specimens for 72h in a desiccator with silica gel at 50°C. Therefore, most of the moisture could be removed while minimising the effects of physical ageing. Oxidative reactions were also minimised by appyling vacuum to the desiccator. In order to keep track of the correct initial water uptake and provide a consistent comparison basis for specimens dried after being immersed, part of the specimens (*Dry* set) was kept in the desiccator for an additional 2500h, after which a moisture-free state was reached and physical ageing processes were considered to be stabilised

[3].

From the unaged state, sets of specimens were immersed in demineralised water at 50°C for 500h, 1000h, 1500h and 4800h (*Saturated* set) according to Procedure A of the ASTM D5229/D5229M standard. This particular temperature was chosen based on DSC test results conducted on saturated resin material. Since DSC specimens are small blocks of material, their short saturation time allows for a quick determination of the wet glass transition temperature (T_g). For the resin system considered in this work, the wet T_g was approximately 70°C (see Section 3.4 and Table 6 for details) and since the material behaviour changes drastically after this threshold, a safety temperature margin of 20°C was adopted. The effect of changing the immersion temperature on the diffusion process and material degradation is well documented in the literature [7, 10, 12] and is out of the scope of this work.

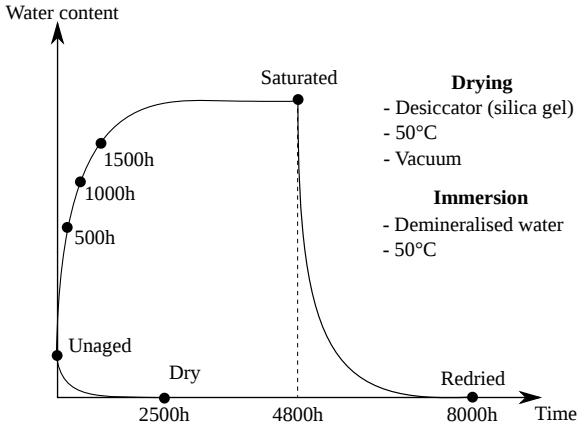

Figure 1: Overview of conditioning procedures.

From the saturated state, a final set of specimens was redried in the desiccator at 50°C until weight stabilisation was reached (*Redried* set). These specimens are used to investigate the possibility of mass loss or residual water after drying and to provide a measure of the irreversible material damage brought by immersion. As the drying process is long and may involve additional physical ageing, the results of this set were compared with the ones from the *Dry* set for consistency.

2.3. Material Investigations

An overview of the mechanical and thermal tests performed for each condition and specimen type can be seen in Table 1, where the number of specimens used for each set is indicated in parentheses. Composite short-beam specimens with 4 and 6 plies were tested in three-point bending according to the ISO 14130

standard in an MTS test frame with a 10kN load cell. Quasi-static tests were conducted in displacement control at a speed of 1mm/min until a significant load drop was observed. Fatigue tests were conducted only on 6-ply specimens in a compression-compression setup in load control at 3Hz, with an R-value of 10.

	Unaged	500h	1000h	1500h	Saturated	Dry	Redried
ILSS	$C_4S(12)/C_6S(12)/C_6F(7)$	$C_4S(3)$	$C_4S(3)$	$C_4S(3)$	$C_4S(6)/C_6S(6)/C_6F(6)$	$C_4S(6)/C_6S(6)$	$C_4S(6)/C_6S(6)$
Tension	ES(6)/EF (5)	-	-	-	ES(6)/EF(9)	ES(6)	ES(6)
Bending	ES(6)	-	-	-	ES(6)	ES(6)	ES(6)
DMA	E(6)	-	-	-	E(6)	E(6)	E(6)
DSC	E(3)	-	-	-	E(3)	E(3)	E(3)
Optical	-	-	-	-	$C_4(3)/C_6(3)$	$C_4(3)/C_6(3)$	-

C_4 - Composite (4-ply), C_6 - Composite (6-ply), E - Neat Epoxy, S - Quasi-static, F - Fatigue

Table 1: Overview of the performed investigations for each condition. The number of specimens for each set is indicated in parentheses.

Resin dog-bone specimens were tested quasi-statically in tension at a speed of 1mm/min and in tension-tension fatigue at 2Hz with an R-value of 0.1. In order to accurately measure strains in quasi-static tests, strain gauges were used both in longitudinal and transverse directions. Neat epoxy bending specimens were also tested using the same fixture mentioned for composite ones. For these tests, a 1kN load cell was used to measure force. In this case, only quasi-static tests were performed, at a speed of 2mm/min.

Dynamic Mechanical Analysis (DMA) tests were conducted in neat epoxy bending specimens by applying a displacement-controlled tension-compression cyclic load with an amplitude of 0.1 mm and a frequency of 1Hz. At the same time, a temperature ramp was applied to the specimen, from 25°C to 130°C at a rate of 2°C/min. After logging the obtained force readings for the complete temperature ramp, the procedure outlined in the standard ISO 6721-5 was used to obtain measurements of the storage and loss moduli, as well as the loss factor. Then, by observing variations in the storage modulus as temperature increases, an estimate of the glass transition temperature was obtained.

Differential Scanning Calorimetry (DSC) tests were performed on resin specimens using a Netzsch DSC 200 F3 Maia apparatus. In the tests, small material blocks are subjected to a temperature ramp of 20°C/min while having their specific heat capacity measured by a calorimeter. During the ramp, the transition to the rubbery state can be identified by an increase in the energy necessary to maintain the constant temperature ramp as the material requires additional energy to make the transition. Besides providing glass transition

temperature measurements, specific heat capacity peaks around the T_g are indicative of polymer relaxation linked to physical ageing [3].

In order to obtain additional information about the irreversible effects brought by water immersion, the first temperature ramp is followed by an isothermal period of 20 minutes at 130°C to erase the polymer relaxation history (thermal rejuvenation) [3] and completely remove the water molecules inside. The material is then quenched back to room temperature and a second ramp is executed. Results from this second ramp are then used to investigate whether irreversible chain scission or additional crosslinking have occurred during the immersion and drying steps.

Lastly, microscopic observations of dry and saturated composite specimens were made both before and after mechanical tests in order to assess microscopic material failure events occurred during immersion and changes in failure behaviour during the performed tests. Microscopy samples were prepared by cutting slices from specimens along one of their orthotropy planes. The slices were then polished using a Labopol 30 polishing machine by progressively grinding the material with sanding surfaces ranging from 320 to 4000 grit and polishing the final surface using a suspension of diamond particles with an average diameter of $1\,\mu m$. After preparation, the slices were observed in a Motic BA210 optical microscope.

3. Results and Discussion

3.1. Water Uptake and Desorption

The average water uptake curves with time can be seen in Figure 2, where the uptake percentage at time t was calculated as:

$$w(t) = 100 \cdot \left(\frac{m(t) - m_{72}^{\mathrm{u}}}{m_{72}^{\mathrm{u}}} - \frac{m_{72}^{\mathrm{d}} - m_{\mathrm{dry}}}{m_{\mathrm{dry}}} \right) \tag{1}$$

where the reference weight m_{72}^{u} was measured for the *Unaged* set prior to immersion. The points are then adjusted using weight measurements on specimens of the *Dry* set, which were dried until a moisture-free state was achieved. Thus, the plots do not start at zero but rather at the initial water content level of the unaged specimens. For neat epoxy, both specimen geometries have a similar final uptake of approximately 3.94%. In the curves for composite specimens, a difference in uptake speed is observed between the thinner 4-ply and the thicker 6-ply specimens, as expected. Eventually, they both attain the same final uptake of approximately 1.25%.

Water transport in polymers and polymer matrix composites is often modelled as Fickian, represented

by a smooth molecular flux $\mathbf{J}$ driven by a concentration gradient with components given by:

$$J_s = -D_s \frac{\partial c}{\partial s} \tag{2}$$

where c is the water concentration field and J_s and D_s are the flux component and diffusivity in the s direction, respectively. By considering all flux components in an infinitesimal material volume, the concentration variation with time ($\partial c/\partial t$) can be obtained via:

$$\frac{\partial c}{\partial t} = \mathbf{D}\nabla^2 c \tag{3}$$

with ∇^2 being the Laplace operator with respect to the spatial coordinates and $\mathbf{D}$ is the diffusivity matrix, which is usually considered orthotropic for unidirectional fibre-reinforced polymer specimens.

Equation 3 is usually solved analytically for the simple case of unidimensional diffusion [7, 15, 18], a suitable approach for specimens such as panels, where the thickness is considerably smaller than the other dimensions. Here, such assumption is not valid and the contribution of all three dimensions must be considered. Instead of resorting to analytically solving Eq. 3, the Finite Element Method can be used to solve it numerically by dividing the spatial domain in finite elements and solving the weak integral form of the problem:

$$\mathbf{K}\mathbf{c} + \mathbf{C}\dot{\mathbf{c}} = \mathbf{f} \tag{4}$$

where $\mathbf{c}$ and $\dot{\mathbf{c}}$ are now nodal vectors of concentration and its variation with time, $\mathbf{K}$ is a diffusion matrix which depends on the shape functions and on the diffusivity matrix $\mathbf{D}$, $\mathbf{C}$ is a capacity matrix that depends only on the shape functions and $\mathbf{f}$ is a vector of externally applied water fluxes.

Each specimen type is meshed with 512 8-node hexahedrical finite elements and the concentration at every boundary node is prescribed to be the final uptake w_∞. Finally, the uptake curve is obtained by averaging the concentration field in the whole volume of the specimen at each time step.

In order to fit the experimental data using the proposed model, suitable values for the diffusivity coefficients in each direction (D_x, D_y and D_z) and the maximum uptake (w_∞) have to be found. In order to evaluate the quality of the fit, the sum of the squared differences between experimental (w_{exp}) and numerical (w_{num}) uptakes is used and cast as a function f of the model parameters:

$$f\left(\mathbf{D}, w_\infty\right) = \sum_t \left[w_{\text{exp}}\left(t\right) - w_{\text{num}}\left(\mathbf{D}, w_\infty, t\right) \right]^2 \tag{5}$$

The problem of identifying the parameter set that produces the best fit can be seen as an optimisation problem in which we seek to minimise the function f subjected to the variable bounds $D_x, D_y, D_z, w_\infty \geq 0$

and to the transverse isotropy condition $D_y = D_x$. Furthermore, for neat resin specimens, complete isotropy is assumed ($D_z = D_x$) while for composites the following relationship is considered [23]:

$$D_z = D_x \cdot \frac{(1 - V_f)}{\left(1 - 2\sqrt{V_f/\pi}\right)} \tag{6}$$

in order to account for the faster diffusion along the fibres, where V_f is the fibre volume fraction. It is important to note that such expression does not account for eventual capillarity effects but only for the geometric effect of fibres acting as obstacles and hindering the diffusion process in the x and y directions. For the laminate considered in this work, $V_f = 0.46$ (obtained through loss on ignition) and therefore $D_z = 2.3D_x$. The problem can then be solved for D_x and w_∞ using a quasi-Newton nonlinear optimisation algorithm.

The parameter identification results can be seen in Figure 2 and Table 2 (labelled *Optimised* w_∞), where the value of f was adimensionalised with respect to w_∞ to produce relative differences. For neat resin, a good fit was obtained for both specimen types and the identified value of w_∞ coincided with the experimentally obtained one. This indicates that the resin behaviour can be correctly represented by Fick's law. For composite specimens, high relative errors were found at long immersion times, as can be seen in plots (b) and (c) of Figure 2, suggesting the occurrence of non-Fickian absorption processes. The same conclusion is reached if the value of w_∞ is fixed at the maximum experimental value and the optimisation problem is used to find only D_x (with label *Maximum* w_∞), with the fit being better at longer times but worse at shorter times, with an overall higher value for f.

Even though an accurate Fickian fit cannot be obtained for the complete curves of the composite samples, closer inspection of the 4-ply curve shows an apparent saturation at 1.19% between 1000h and 2000h, suggesting that the absorption behaviour takes place in two distinct phases. Fixing $w_\infty = 1.19\%$ and optimising for D_x (*Adjusted* w_∞), a very close fit is obtained for the first 2000h, shown as the f value inside parantheses in Table 2. This first absorption phase can therefore be considered as Fickian and is followed by a secondary time-dependent phase. For 6-ply specimens, the same adjusted value of $w_\infty = 1.19\%$ also gives a good fit for the early phase of fast water uptake and an underestimate for the later phase. It is concluded that water uptake on composite specimens is not a purely Fickian process. This can be indicative for topological changes in the material microstructure.

Figure 3 shows specimen weights measured during the desorption process for both neat resin and composite, a process that took approximately 3200h. Both types of composite specimens showed weight loss (0.15% loss for 4-ply and 0.06% loss for 6-ply specimens). Such material loss was also observed by other

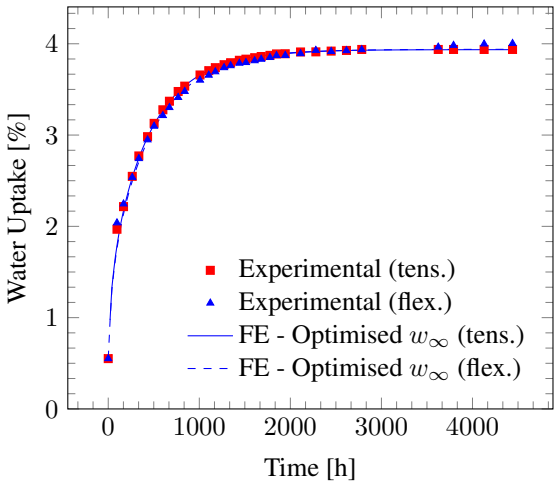

(a) Neat resin specimens

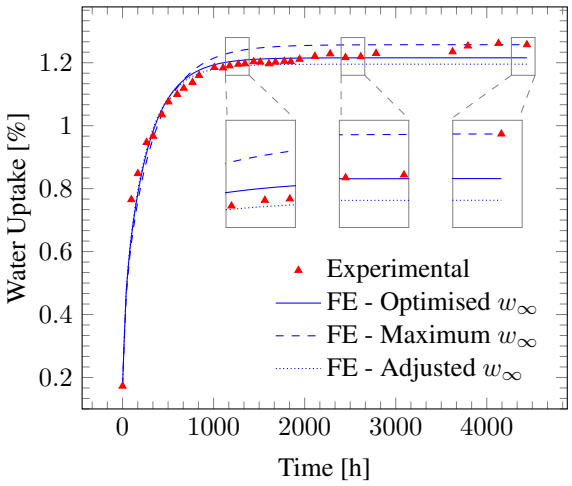

(b) 4-ply composite specimens

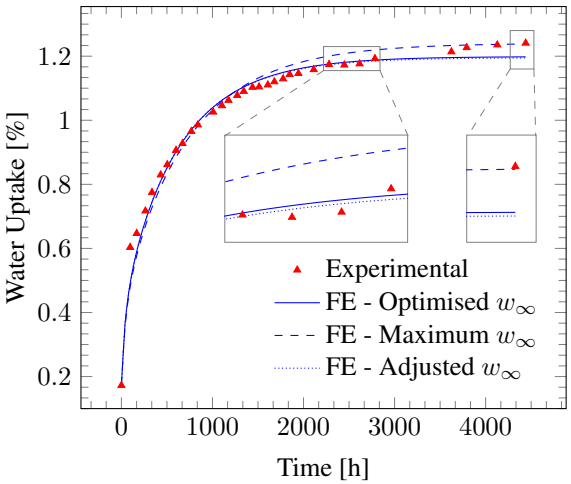

(c) 6-ply composite specimens

Figure 2: Water uptake values and Fick's law fit. Each point is an average of measurements in three specimens.

	Optimised w_∞				Maximum w_∞		Adjusted w_∞	
	Tens.	Flex.	4 plies	6 plies	4 plies	6 plies	4 plies	6 plies
D_x $(\cdot 10^{-13})$ $[m^2/s]$	**7.41**	**7.92**	7.84	7.57	6.46	6.43	**8.57**	**7.68**
D_z $(\cdot 10^{-13})$ $[m^2/s]$	**7.41**	**7.92**	18.03	17.41	14.86	14.79	**19.71**	**17.67**
w_∞ [%]	**3.94**	**3.94**	1.21	1.20	1.26	1.24	**1.19**	**1.19**
f/w_∞^2 $(\cdot 10^{-2})$ [-]	0.33	0.15	1.24	1.18	3.05	1.89	1.84 (0.74)	1.21 (0.01)

Table 2: Uptake curve fitting results, with adopted values shown in bold.

authors [7, 12, 17], particularly when high immersion temperatures are used, and is usually attributed to leaching of hydrolised components from the bulk resin and interphase regions.

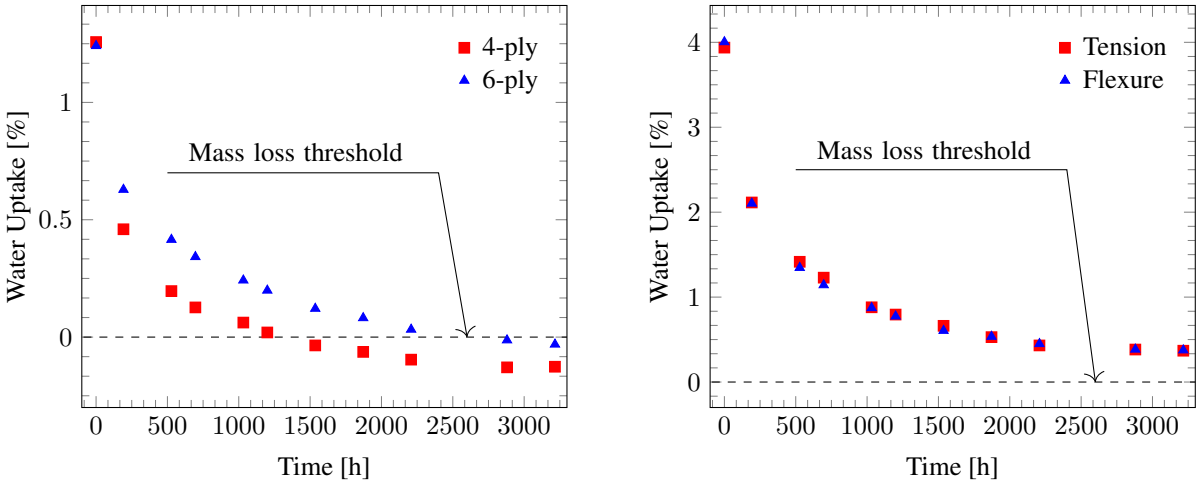

(a) Composite

(b) Neat resin

Figure 3: Water desorption curves showing weight loss for composites and residual uptake for resin

For neat resin, on the other hand, a residual water uptake of 0.31% was observed at equilibrium, suggesting that part of the water could not be removed through drying at 50°C. Such behaviour was also observed by Zhou and Lucas [5], who describe two types of chemical bonds which occur between water molecules and epoxy polymer chains. Type I bonds have a lower activation energy and are readily removed through drying, but type II bonds have higher energy and require higher drying temperatures in order to be removed. Two out of the three types of epoxy considered by Zhou and Lucas [5] showed a residual uptake of approximately

0.30% after immersion and drying at 60°C, while the third one retained 0.18% of the absorbed water. The results obtained in this work seem to confirm the existence of such stronger bonds. Furthermore, irreversible water uptake in neat resin implies that the actual amount of material washed away in composite specimens is higher than what follows directly from weight loss measurements.

3.2. Mechanical Tests

In order to investigate the evolution of the composite material degradation during water uptake, sets of 4-ply ILSS specimens were tested after 500h, 1000h and 1500h of immersion and at saturation. Figure 4 shows stress-displacement curves for specimens tested after each immersion time. To avoid clutter, only one representative curve was chosen from each set. Also shown is the evolution of strength plotted together with the measured water uptake values.

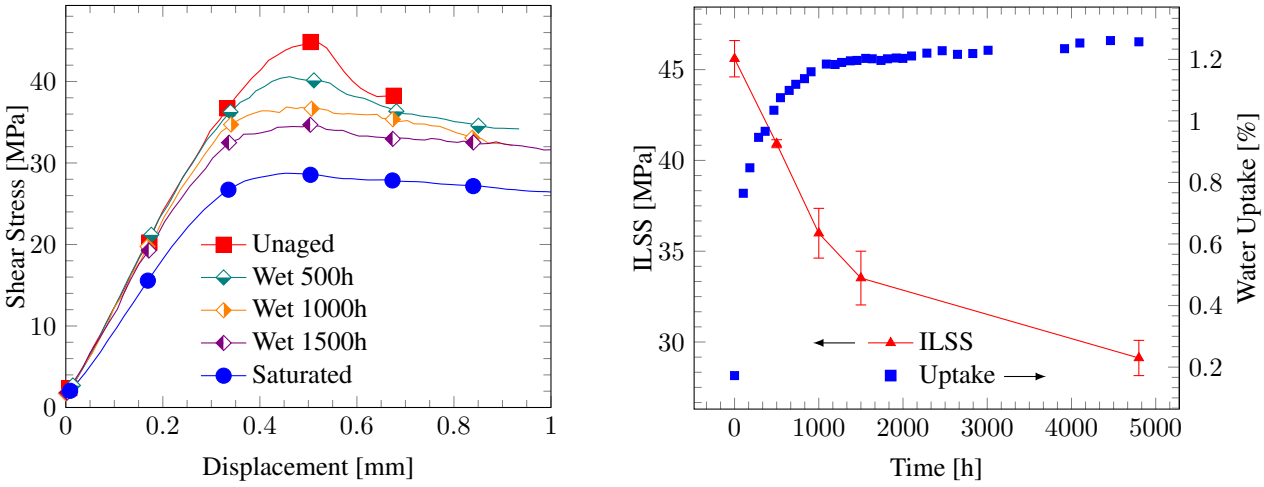

Figure 4: Static ILSS results for specimens immersed for multiple durations (4-ply composites).

From the results, material degradation both in terms of stiffness and strength can be observed, with up to 36% strength reduction. Such degradation is usually attributed to the combined effect of hydrolytic attack on both the resin and the silanic coupling agent around the fibres [24], differential swelling between fibre and matrix [11] and matrix plasticization [2]. By conducting both mechanical and thermal tests and fractographic observations, the relative contributions of each of these mechanisms will be assessed throughout the rest of this paper.

Closer inspection of the stress-displacement curves of Figure 4 suggests that the failure behaviour becomes more ductile as immersion time increases, with gradual load drops instead of the more sudden drops

observed in reference specimens, suggesting the occurrence of matrix plasticization. Regarding the evolution of strength with immersion time, it can be seen that the degradation keeps increasing well beyond the apparent saturation phase between 1000h and 2000h. This suggests that degradation is not only a function of water uptake but is also time-dependent. Two distinct mechanisms may be suggested as being responsible for such behaviour. Firstly, hydrolytic chemical reactions and subsequent leaching of material at the fibre/matrix interfaces lead to a weakening of the interfacial bond and creation of additional spaces for water uptake [8]. Secondly, differential swelling stresses [11, 25] at the weakened interfaces promote crack initiation and propagation, further increasing the available space for water uptake. It is important to note that such mechanisms may act in isolation or in combination, synergistically reinforcing one another.

Results for 6-ply specimens can be seen in Figure 5, for which a 34% strength reduction was observed, with similar failure behaviour when compared to the 4-ply specimens. In this case, stress-displacement curves for all specimens are shown. Results for both specimen types can also be seen in Table 3.

For fatigue, S-N curves were obtained by fitting the experimental data to a straight line in log-log space given by:

$$\log_{10} N = A + B \cdot \log_{10} |\tau_{\max}| \tag{7}$$

where N is the number of cycles before failure occurs, $|\tau_{\max}|$ is the absolute value of the maximum attained shear stress and A and B are the intercept and slope parameters, respectively. From the obtained curves, it can be observed that conditioned specimens suffered a fatigue life reduction of three orders of magnitude for a given load level, while the maximum stress showed decreases of approximately 40% for a given number of cycles, a degradation level similar to the one obtained in the static tests.

	Unaged	500h	1000h	1500h	Saturated	Dry	Redried
4 plies							
$\tau_{\max}$ [MPa]	45.6 ± 1.0	40.9 ± 0.2	35.9 ± 1.4	33.5 ± 1.5	29.1 ± 0.9	53.7 ± 1.6	44.6 ± 1.3
6 plies							
$\tau_{\max}$ [MPa]	46.1 ± 1.3	-	-	-	30.3 ± 1.1	52.3 ± 1.8	41.7 ± 1.0

Table 3: ILSS values of composite specimens for every type of conditioning.

Although interlaminar shear fatigue results after hygrothermal ageing for the current material system could not be found in literature, a limited comparison can be made with works dealing with other resin

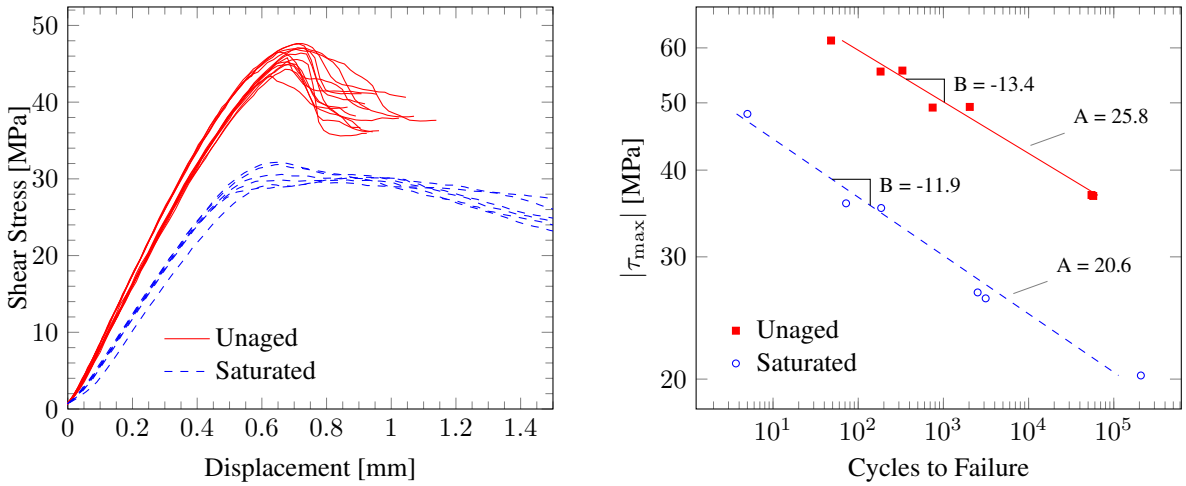

Figure 5: Static and fatigue ILSS results for unaged and saturated specimens (6-ply composites).

systems or test types. Hu et al. [1] reported 90° tension-tension fatigue results on the same glass/epoxy system used in this work, with strength reductions of up to 44% for low cycle tests, similar to the present results. As 90° tension and interlaminar shear tests are both dominated by a combination of resin and interface properties, similar levels of degradation were expected. However, a drastic slope reduction was obtained by the authors, resulting in near-horizontal S-N curves for wet samples and seemingly no effect of ageing in high cycle tests. Such behaviour, which was also reported by Vauthier et al. for a different glass/epoxy system [19], was not observed here.

In order to investigate the relative contributions of interface and matrix damage after immersion, neat epoxy specimens were tested in tension and bending. Stress-displacement curves for reference and conditioned specimens are shown in Figures 6 and 7, while average results can be seen in Tables 4 and 5. For both specimen types, the Young's modulus and strength decreased by approximately 17% after saturation. A slight change in failure mode was also noticed for tension specimens, as can be seen in Figure 10, with saturated specimens showing a markedly ductile behaviour with extensive necking. In fatigue, the number of cycles to failure decreased by two orders of magnitude for a given stress level and a slightly steeper slope was obtained, which is again opposite to the behaviour observed by other authors [1, 19].

Here, two possible major degradation mechanisms exist, namely plasticization and breakage of polymer chains through hydrolytic reactions. While the more ductile failure mode suggests that plasticization is the main effect, the thermal tests of Section 3.4 will be used to confirm this hypothesis. Comparing results

of resin and composite specimens, it can be seen that the observed magnitude of resin degradation (17%) is not enough to explain the one obtained for composites (35%), indicating that interfacial hydrolysis and differential swelling play an equally important role in the total property reduction.

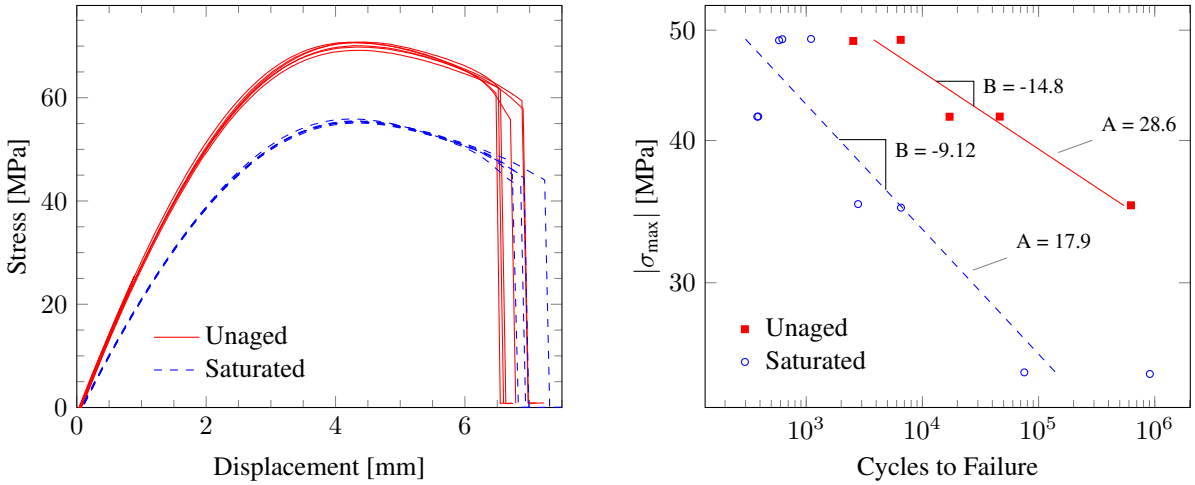

Figure 6: Static and fatigue tension results for unaged and saturated specimens (neat resin).

	Unaged	Saturated	Dry	Redried
σ_{max} [MPa]	70.3 ± 0.6	55.5 ± 0.3	72.2 ± 0.3	58.1 ± 11.5
ϵ at σ_{max} [%]	4.53 ± 0.05	4.35 ± 0.08	4.53 ± 0.05	2.71 ± 1.05
ν [-]	0.381 ± 0.010	0.399 ± 0.018	0.382 ± 0.007	0.374 ± 0.011
E [GPa]	3.15 ± 0.06	2.53 ± 0.07	3.06 ± 0.03	3.05 ± 0.03

Table 4: Results of tension tests in neat epoxy specimens for every type of conditioning.

As both differential swelling and softening effects caused by plasticization are reversible upon moisture removal, tests on redried specimens are useful in order to isolate the contribution of the non-reversible mechanisms. As mentioned in Section 2.2, results from the *Redried* set will be compared with those from the *Dry* set, since both are tested after complete drying at 50°C and after stabilisation of polymer relaxation processes. Figures 8 and 9 show stress-displacement curves for both sets, with average results shown in Tables 3, 4 and 5.

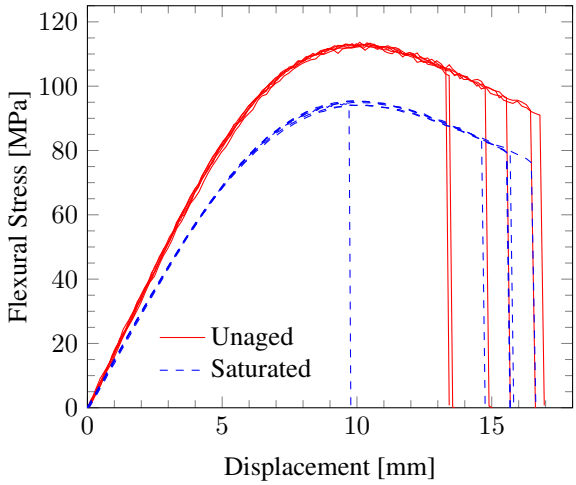

Figure 7: Static bending results for unaged and saturated specimens (neat resin).

	Unaged	Saturated	Dry	Redried
$\sigma_{\text{flex,max}}$ [MPa]	113.8 ± 0.4	95.1 ± 0.6	116.2 ± 0.7	113.8 ± 1.4
ϵ at $\sigma_{\text{flex,max}}$ [%]	5.98 ± 0.12	5.85 ± 0.09	5.84 ± 0.08	5.89 ± 0.11
E_{flex} [GPa]	2.88 ± 0.23	2.47 ± 0.03	3.03 ± 0.02	3.03 ± 0.10

Table 5: Results for bending tests in neat epoxy specimens for every type of conditioning.

For composites, an irreversible shear strength degradation of 17% for 4-ply and 20% for 6-ply specimens was found, with similar permanent reductions observed for the shear stiffness. This irreversible degradation indicates a significant contribution of the combined effect of hydrolytic interface weakening and cracking driven by differential swelling stresses, a process which is also consistent with the observed non-Fickian absorption uptake phase and the mass loss upon drying.

It is also important to investigate the resin behaviour after redrying, since any irreversible effects on the resin will also impact the composite behaviour. Here, in contrast to previous observations, the effect on stiffness is markedly different from the one on strength and fracture behaviour. For both tensile and bending specimens, a complete recovery of stiffness was obtained after drying. However, a transition from ductile to brittle failure behaviour was observed (Figure 10). This effect can be observed for bending specimens in the form of a lower strain at failure for redried specimens, but is much more drastic for tensile specimens,

with only one specimen out of six reaching the end of the plastic hardening regime and sudden failure with a large amount of scatter for all other specimens.

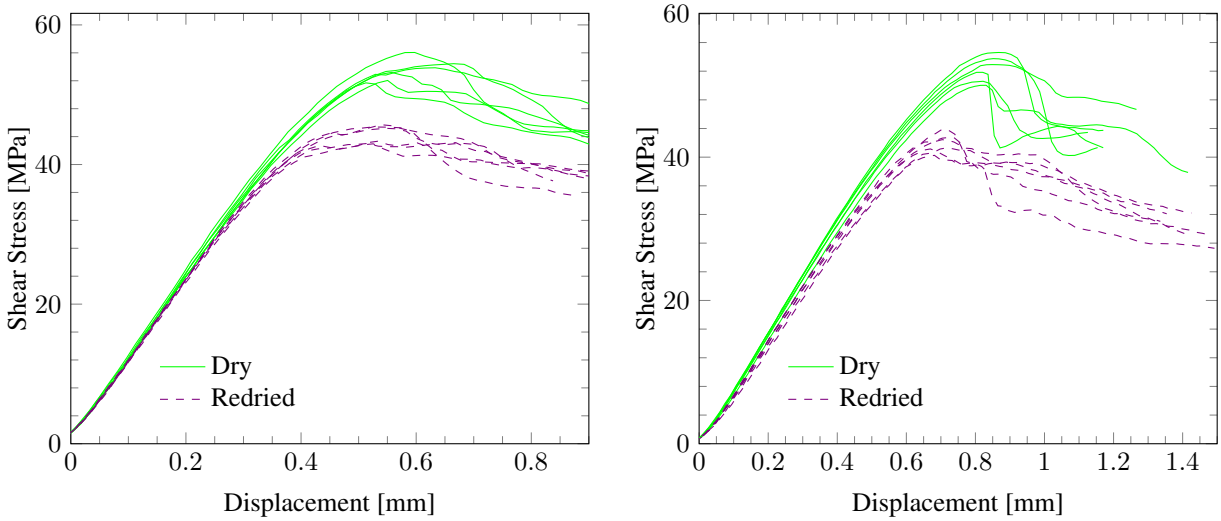

(a) 4-ply specimens

(b) 6-ply specimens

Figure 8: Static ILSS results for dry and redried specimens (4-ply and 6-ply composites) .

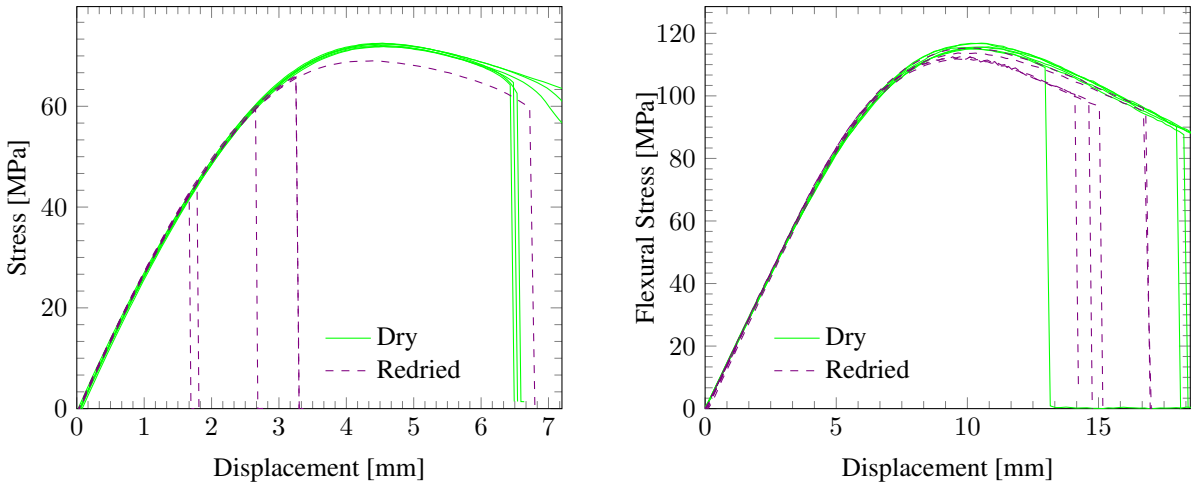

(a) Tension

(b) Flexure

Figure 9: Static tension and bending results for dry and redried specimens (neat resin).

Assuming that the possibility of post-curing and chain breakage during the immersion and redrying

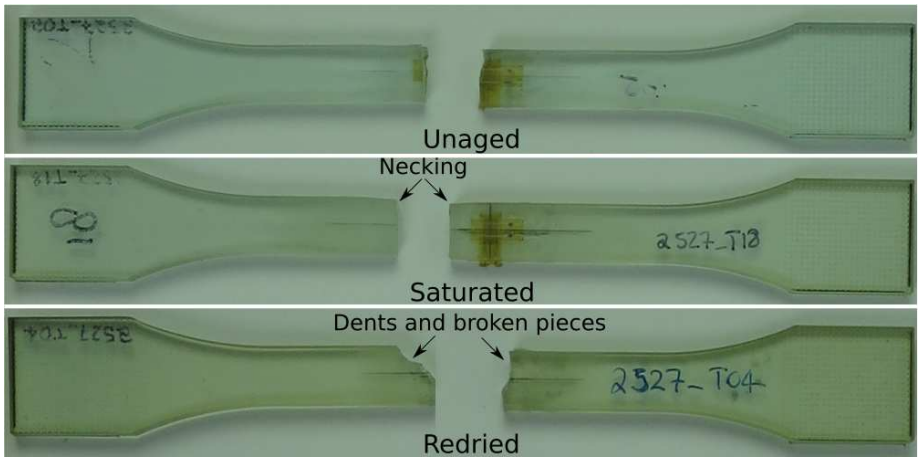

Figure 10: Change of failure pattern between unaged, saturated and redried tension specimens.

steps can be ruled out (see Section 3.4 for details), two explanations can be proposed for the observed decrease in the strain at failure. First, even though both specimen sets were given enough time for polymer relaxation to happen until stabilisation [3], the movement of water molecules during the uptake-desorption cycle experienced by the redried specimens may have modified their free volume structure, as argued by Wong and Broutman [9], which would bring changes to their fracture behaviour. Second, the residual water retained in the specimens after redrying may be promoting secondary crosslinks between polymer chains, as proposed by Zhou and Lucas [5]. Such stronger link between the water molecules and polymer chains also helps explaining why they require a higher energy in order to be removed.

3.3. Microscopic Observations

Composite specimens from the *Dry* and *Saturated* sets were inspected using an optical microscope both before and after being tested. The inspections conducted before testing were carried out to find evidences of material degradation from immersion, while the ones conducted after testing investigated changes in failure behaviour caused by such degradation.

Figure 11 shows x-y plane views of a dry and a saturated specimen (plies are stacked along the z axis). After immersion, the fibre bundles, which were barely visible in reference specimens, can be visually identified, suggesting that interface debonding took place. In particular, this is visible in the areas marked (a) and (b), showing debonding in fibres oriented both in 0° and 90° directions. Figure 12 shows views of the x-z plane of two different saturated specimens at two different points along their thickness. In the pictures,

the fabric stitches can be seen as shadows in the spaces between two consecutive plies and are indicated in white. In both pictures, regions of intact and darkened fibres can be identified, with the latter being marked by arrows. Such darkened fibres are indicative of cracks running along the interfaces and are considered as a sign of weak interface adhesion since they do not propagate to the surrounding resin [26, 27]. These observations reinforce the hypothesis that the combination of high differential swelling stresses and a weakened interface cause cracks to propagate along them and create new loci for water absorption.

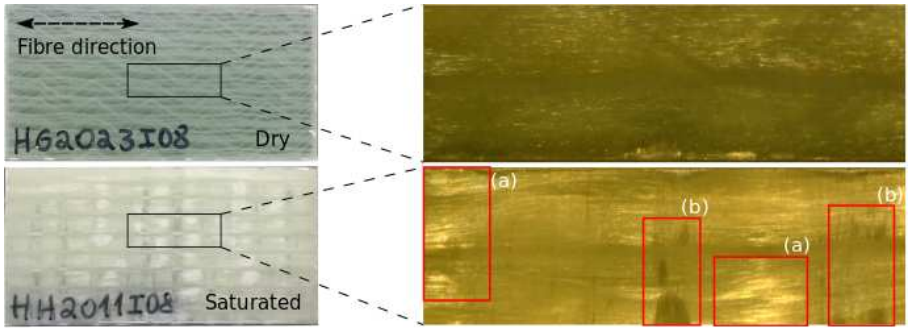

Figure 11: In-plane microscopic comparison of dry and saturated specimens, with (a) debonding in the 0° direction and (b) debonding in the 90° stabilization roving.

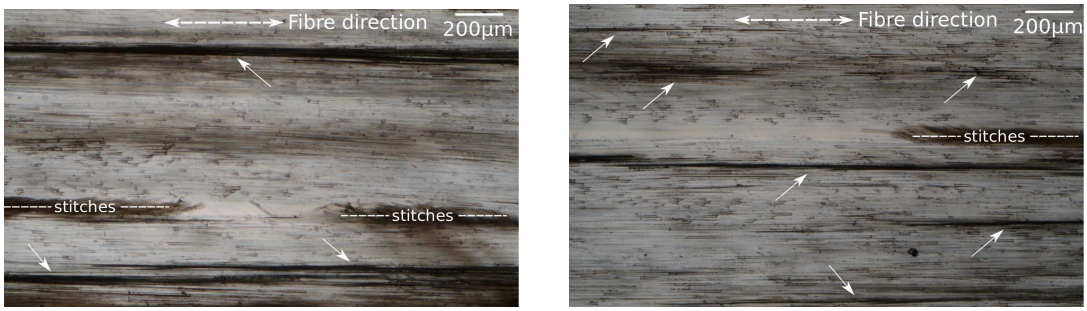

Figure 12: Through-thickness micrographs of a saturated specimen with arrows indicating debonded regions.

Figures 13 and 14 show y-z views of dry and saturated specimens after being tested in three-point bending, with the fibre direction oriented out of plane. The general failure behaviour is the same for both condition types, with longitudinal shear cracks running through the whole width of the specimens. For dry specimens, a single crack or a pair of symmetric cracks is observed around the fibre bundle located at mid-thickness, where the material experiences the maximum value of shear stress. For saturated specimens, on the other hand, cracks occur at multiple locations, including in regions close to the specimen surfaces, as

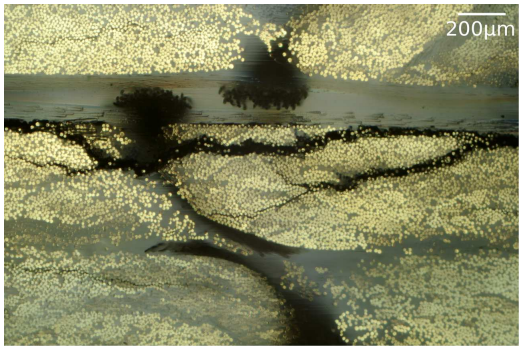

(a) Crack propagation through fibre bundles

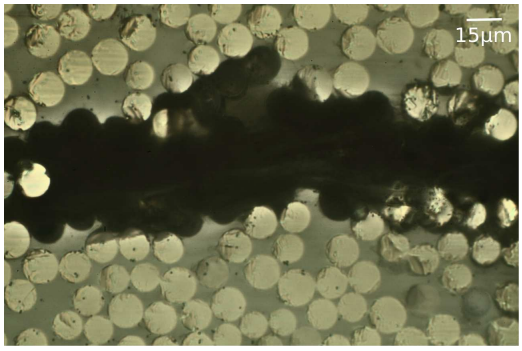

(b) Detail of the crack surface

Figure 13: Microscopic observation of the crack surfaces of a dry specimen after testing.

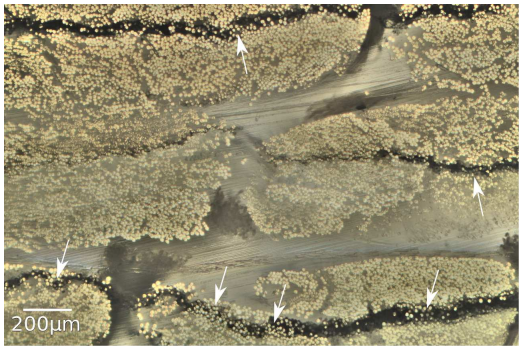

(a) Crack propagation through fibre bundles

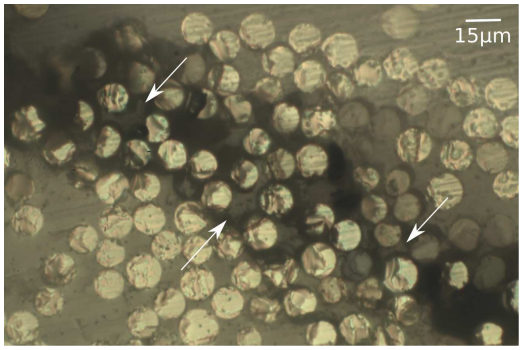

(b) Detail of the crack surface

Figure 14: Microscopic observation of the crack surfaces of a saturated specimen after testing, with arrows indicating regions of predominant plastic resin failure.

shown in Figure 14a. This observation is consistent with the fact that regions closer to the surfaces were the first to get saturated and therefore the ones exposed for the longest time to the time-dependent degradation mechanisms mentioned in Section 2. The crack propagation behaviour was also different between dry and saturated specimens. In dry samples, the main crack tends to run along the boundaries of fibre bundles, with secondary cracks moving inside the bundles being arrested. In saturated samples, the cracks tend to run inside the bundles, where differential swelling creates high stress concentrations.

Finally, upon further investigation of the crack surfaces at higher magnifications, more differences between dry and saturated specimens become apparent. Crack surfaces in dry specimens suggest a failure dominated by clean fibre/matrix interface debonding (Figure 13b). For saturated specimens, at multiple

points along the cracks (marked with arrows in Figure 14a), damage was more distributed, with the presence of resin fragments between fibres (marked areas in Figure 14b), suggesting that the main crack was formed by the propagation and coalescence of multiple smaller interface cracks. This reinforces both hypotheses of a plasticized resin and a weakened fibre/matrix interface after immersion and the consequent crack arrest mechanisms explain the increasingly ductile material behaviour as more water is absorbed (Figure 4).

3.4. Thermal Tests

Figure 15 shows storage modulus curves obtained through DMA testing, where the crossing of tangents to the inflection points in the storage modulus curve is considered to be the glass transition temperature (T_g) of the resin. Loss factor curves are also plotted and peak values are marked (T_{fp}). Average values are reported in Table 6. In saturated specimens, the measured glass transition temperature was on average 17°C lower than in *Unaged* specimens. Such decrease is in line with the observed decreases in stiffness and strength of the resin, since it also points to the occurrence of matrix plasticization.

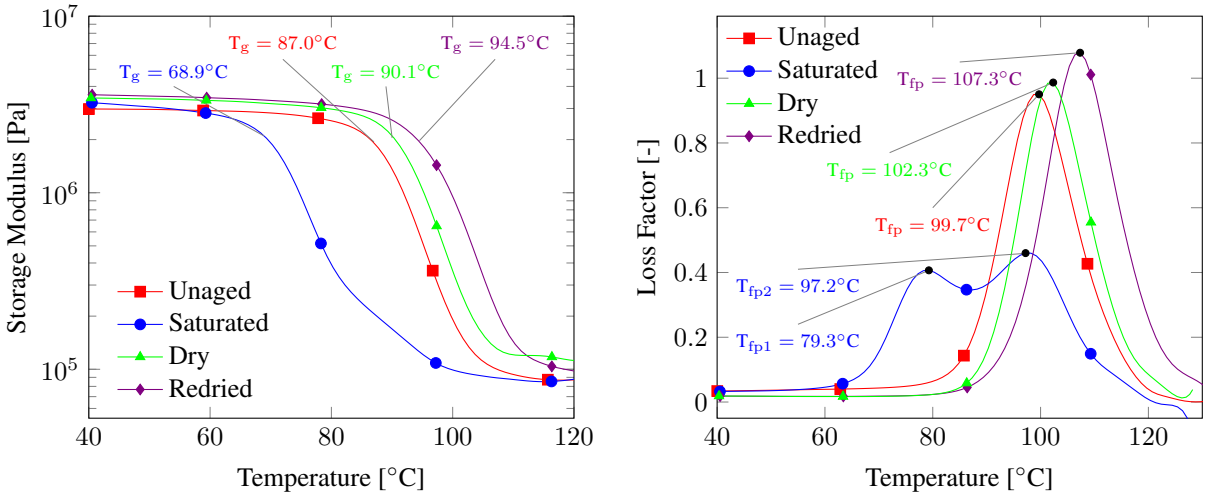

(a) Storage modulus

(b) Loss Factor

Figure 15: DMA results for every type of conditioning (neat resin).

Comparing results from the *Dry* and *Redried* sets, previous exposure to moisture resulted in an increase of 4°C to the measured T_g, which agrees with the observed change to brittle failure modes in mechanical tests. As an increase in T_g is expected both in the case of additional crosslinking and polymer relaxation associated with a reduction of specific free volume [3], the results observed here support the hypothesis

	Unaged	Saturated	Dry	Redried
Dynamic Mechanical Analysis (DMA)				
T_{g} [°C]	86.8 ± 0.3	70.0 ± 0.6	90.3 ± 0.4	94.3 ± 0.4
T_{fp} [°C]	99.1 ± 0.5	80.3 ± 0.8 & 98.9 ± 1.1	101.9 ± 0.4	107.4 ± 0.4
Differential Scanning Calorimetry (DSC)				
T_{g1} [°C]	86.6 ± 0.3	69.3 ± 0.5	90.1 ± 1.7	87.9 ± 2.5
T_{g2} [°C]	90.1 ± 0.8	88.2 ± 0.5	89.4 ± 1.2	89.0 ± 0.3
Δh [J/g]	1.44 ± 0.55	6.16 ± 0.48	2.99 ± 0.45	2.64 ± 0.31

Table 6: Thermal analysis results on neat resin.

that these processes can explain the decrease in strain at failure discussed in Section 3.2. Similar changes were observed for the loss peak temperature, although a second peak is observed for the *Saturated* set. This phenomenon was also observed by other authors [14, 28], who attributed it to a phase change of water molecules not attached to the polymer structure. However, since the temperature for the second peak is similar to the one for *Unaged* samples, it may also point to the presence of unplasticized polymer chains in the saturated material.

Figure 16 shows Differential Scanning Calorimetry (DSC) curves for one representative specimen of each set. To facilitate the comparison between specimens, the curves were scaled based on the heat capacity value at 140°C. The main conclusion here comes by considering the results from the second heat cycle, after the specimens were kept at 130°C in order to erase their polymer relaxation history and remove residual water molecules. The T_{g2} of specimens for all conditions, measured at the onset of the phase change, was the same, indicating that no additional monomer-hardener crosslinks occurred during drying or redrying of the samples and that chain breakage through hydrolysis was not significant during immersion.

Finally, T_g measurements are also taken during the first heating cycle. As expected, T_{g1} values of saturated specimens were lower than those of the other sets due to the presence of plasticized polymer chains. However, comparing the *Dry* and *Redried* sets, no significant difference in T_{g1} was found, in contrast to the results obtained with DMA tests. As the first cycle usually includes an enthalpy relaxation peak caused by physical ageing occurred during manufacturing and conditioning, it is also interesting to evaluate their magnitudes (Δh) by subtracting the first and second cycle curves and taking the area below the resultant

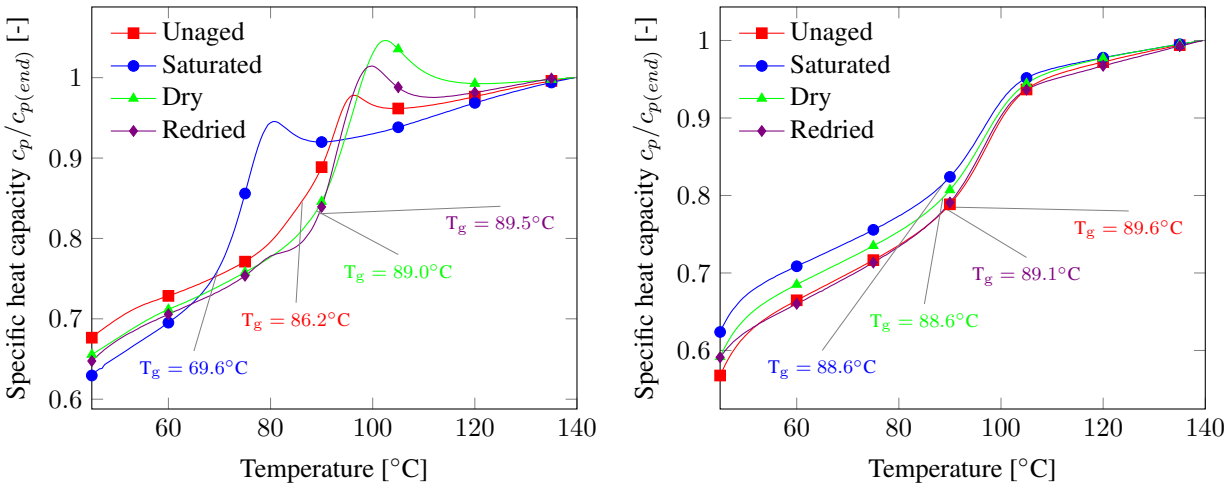

(a) First heating cycle

(b) Second heating cycle

Figure 16: DSC results for every type of conditioning (neat resin).

curve in a 30°C temperature range starting at the glass transition onset. As the *Unaged* condition was chosen in order to minimise the effects of polymer relaxation, an expected increase in Δh is observed for *Dry* and *Redried* samples. Differences were also observed between the two dry sets, indicating differences in their polymer structure and agreeing with DMA and mechanical test results. Lastly, the relaxation of *Saturated* specimens was the highest and can be associated with the combined phase change of the resin and unbounded water molecules.

4. Conclusions

This work investigated material degradation effects caused by hygrothermal ageing in composite and neat epoxy specimens for a fibre and resin system representative of the material used in wind turbine blades. Water uptake and desorption behaviours were investigated. Specimens were conditioned in hot water (50°C) for 4800h, dried after having been immersed and isothermally dried without immersion. Static and fatigue properties of aged and unaged specimens were measured and compared. Additionally, a combination of thermal analytical techniques and optical microscopy was used in order to explain the relative contributions of each degradation effect.

An optimisation-based parameter identification procedure was used to fit a 3D Fick finite element model to the measured uptake data. For neat resin, the behaviour was Fickian, while for composites it was com-

posed of an initial Fickian phase followed by a secondary non-Fickian absorption phase at longer immersion times. Upon redrying, composite specimens showed weight loss linked to the combined action of interface decomposition and crack propagation driven by differential swelling stresses with subsequent leaching of material. For neat resin specimens, part of the water could not be removed through redrying, an evidence suggesting that part of the water molecules form stronger bonds with the polymer network [5] and that the material loss observed for composite specimens is higher than what follows from weight measurements.

Material degradation in composite specimens as measured through mechanical tests was not only dependent on the water uptake but also on immersion time, with shear strength reductions of up to 36% and fatigue life up to three orders of magnitude shorter. For resin specimens, a degradation level of approximately 17% was observed, both in tension and in bending. After redrying, an irreversible mechanical property reduction of 17% was found for composite samples, while for resin the stiffness and maximum attainable stress are fully recovered and a notable decrease in the strain level at failure is observed. Even though different test types were used in the comparison between composite and resin, the observed differences in magnitude and reversibility of degradation strongly indicate that composite degradation cannot be fully explained by only considering mechanisms that act on the resin. Fractographic analysis in unaged composite samples indicated that cracks tend to run along the fibre bundle boundaries and concentrate close to the specimen mid-thickness. For saturated ones, cracks are evenly distributed along the specimen thickness and tend to propagate inside the bundles, suggesting the presence of high differential swelling stresses.

Based on the conducted material investigations, the following chronology is proposed for the hygrothermal ageing process in the present glass/epoxy system: Water diffuses through the material and promotes resin plasticization, degradation of interfacial strength and differential swelling. The combination of the time-dependent weakening of the interfaces with the high differential swelling stresses promotes crack formation along the interfaces and cause additional water uptake in the newly created empty volumes. Upon redrying, the plasticization is reversed and differential swelling subsides, leading to property recovery, although the resin free volume is irreversibly changed and part of the water molecules remain strongly bonded to polymer chains. However, as the irreversible effects on resin specimens do not significantly impact their mechanical behaviour, it can be concluded that the interface cracks formed in composites during uptake are the main reason for the observed permanent reductions in stiffness and strength. With the obtained information about the relative contributions of each degradation effect and their interactions, numerical models can be developed to simulate the ageing process and subsequent material failure during service fatigue loading.

Acknowledgements

The authors acknowledge the contribution of the TKI-WoZ and IRPWIND projects for motivating and partly funding this research and of the TKI-MIMIC project industrial partners for providing useful feedback.

References

[1] Y. Hu, A. W. Lang, X. Li, S. R. Nutt, Hygrothermal aging effects on fatigue of glass fibre/polydicyclopentadiene composites, Polymer Degradation and Stability 110 (2014) 464–472.

[2] L. Gautier, B. Mortaigne, B. V., Interface damage study of hydrothermally aged glass-fibre-reinforced polyester composites, Composites Science and Technology 59 (1999) 2329–2337.

[3] G. M. Odegard, A. Bandyopadhyay, Physical aging of epoxy polymers and their composites, Journal of Polymer Science Part B: Polymer Physics 49 (2011) 1695–1716.

[4] R. Polanský, V. Mantlík, P. Prosr, J. Sušír, Influence of thermal treatment on the glass transition temperature of thermosetting epoxy laminate, Polymer Testing 28 (2009) 428–436.

[5] J. Zhou, J. P. Lucas, Hygrothermal effects of epoxy resin. part I: the nature of water in epoxy, Polymer 40 (1999) 5505–5512.

[6] X. Jiang, H. Kolstein, F. Bijlaard, X. Qiang, Effects of hygrothermal aging on glass-fibre reinforced polymer laminates and adhesive of FRP composite bridge: Moisture diffusion characteristics, Composites: Part A 57 (2014) 49–58.

[7] B. Dewimille, A. R. Bunsell, Accelerated ageing of a glass fibre-reinforced epoxy resin in water, Composites (1983) 35–40.

[8] S. A. Grammatikos, M. Evernden, J. Mitchels, B. Zafari, J. T. Mottram, G. C. Papanicolaou, On the response to hygrothermal ageing of pultruded FRPs used in the civil engineering sector, Materials and Design 96 (2016) 283–295.

[9] T. C. Wong, L. J. Broutman, Water in epoxy resins part II. diffusion mechanism, Polymer Engineering and Science 25 (9) (1985) 529–534.

[10] H. S. Choi, K. J. Ahn, J. D. Nam, H. J. Chun, Hygroscopic aspects of epoxy/carbon fiber composite laminates in aircraft environments, Composites Part A: Applied Science and Manufacturing 32 (2001) 709–720.

[11] Y. Joliff, W. Rekik, L. Belec, J. F. Chailan, Study of the moisture/stress effects on glass fibre/epoxy composite and the impact of the interphase area, Composite Structures 108 (2014) 876–885.

[12] S. A. Grammatikos, B. Zafari, M. C. Evernden, J. T. Mottram, J. M. Mitchels, Moisture uptake characteristics of a pultruded fibre reinforced polymer flat sheet subjected to hot/wet aging, Polymer Degradation and Stability 121 (2015) 407–419.

[13] A. S. Maxwell, W. R. Broughton, G. Dean, G. D. Sims, Review of accelerated ageing methods and lifetime prediction techniques for polymeric materials, Tech. rep., National Physical Laboratory (NPL) (2005).

[14] B. De'Nève, M. E. R. Shanahan, Water absorption by an epoxy resin and its effect on the mechanical properties and infra-red spectra, Polymer 34 (24) (1993) 5099–5105.

[15] G. Pitarresi, M. Scafidi, S. Alessi, M. Di Filippo, C. Billaud, G. Spadaro, Absorption kinetics and swelling stresses in hydrothermally aged epoxies investigated by photoelastic image analysis, Polymer Degradation and Stability 111 (2015) 55–63.

[16] P. Davies, F. Pomies, L. A. Carlsson, Influence of water and accelerated aging on the shear fracture properties of glass/epoxy composite, Applied Composite Materials 3 (1996) 71–87.

[17] P. Davies, F. Mazéas, P. Casari, Sea water aging of glass reinforced composites: Shear behaviour and damage modelling, Journal of Composite Materials 35 (15) (2000) 1343–1372.

[18] F. Ellyin, C. Rorhbacher, Effect of aqueous environment and temperature on glass-fibre epoxy resin composites, Journal of Reinforced Plastics and Composites 19 (2000) 1405–1427.

[19] E. Vauthier, J. C. Abry, T. Bailliez, A. Chateauminois, Interactions between hygrothermal ageing and fatigue damage in unidirectional glass/epoxy composites, Composites Science and Technology 58 (1998) 687–692.

[20] G. Kotsikos, J. T. Evans, A. G. Gibson, J. M. Hale, Environmentally enhanced fatigue damage in glass fibre reinforced composites characterised by acoustic emission, Composites: Part A 31 (2000) 969–977.

[21] E. Poodts, G. Minak, A. Zucchelli, Impact of sea-water on the quasi static and fatigue flexural properties of GFRP, Composite Structures 97 (2013) 222–230.

[22] Technical data sheet - EPIKOTE resin MGS RIMR 135 and EPIKURE curing agent MGS RIMH 134-RIMH 137, Tech. rep., Momentive (2006).

[23] C. H. Shen, G. S. Springer, Environmental effects on composite materials, Technomic, 1981.

[24] L. Salmon, F. Thominette, J. Verdu, M. Pays, Hydrolytic degradation of model networks simulating the interfacial layers in silane-coupled epoxy/glass composites, Composites Science and Technology 57 (1997) 1119–1127.

[25] T. Morii, N. Ikuta, K. Kiyosumi, H. Hamada, Weight-change analysis of the interphase in hygrothermally aged FRP: Consideration of debonding, Composites Science and Technology 57 (1997) 985–990.

[26] C. L. Schutte, W. McDonough, M. Shioya, M. McAuliffe, M. Greenwood, The use of a single-fibre fragmentation test to study environmental durability of interfaces/interphases between dgeba/mpda epoxy and glass fibre: the effect of moisture, Composites 25 (7) (1994) 617–624.

[27] A. Sjögren, R. Joffe, L. Berglund, E. Mader, Effects of fibre coat (size) on properties of glass fibre/vinyl ester composites, Composites: Part A 30 (1999) 1009–1015.

[28] C. Li, R. A. Dickie, K. N. Morman, Dynamic mechanical response of adhesively bonded beams: Effect of environmental exposure and interfacial zone properties, Polymer Engineering and Science 30 (1990) 249–255.